Generation of Coherent X-Ray Radiation Through Modulation Compression

Ji Qiang*
Lawrence Berkeley National Laboratory, Berkeley, CA 94720, USA

Juhao Wu
SLAC National Accelerator Laboratory, Menlo Park, CA 94025, USA

(Dated: March 16, 2011)

In this paper, we propose a scheme to generate tunable coherent X-ray radiation for future light source applications. This scheme uses an energy chirped electron beam, a laser modulator, a laser chirper and two bunch compressors to generate a prebunched kilo-Ampere current electron beam from a few tens Ampere electron beam out of a linac. The initial modulation energy wavelength can be compressed by a factor of $1 + h_b R^a_{56}$ in phase space, where h_b is the energy bunch length chirp introduced by the laser chirper, R^a_{56} is the momentum compaction factor of the first bunch compressor. As an illustration, we present an example to generate more than 400 MW, 170 attoseconds pulse, 1 nm coherent X-ray radiation using a 60 Ampere electron beam out of the linac and 200 nm laser seed. Both the final wavelength and the radiation pulse length in the proposed scheme are tunable by adjusting the compression factor and the laser parameters.

PACS numbers: 29.27.Bd; 52.35.Qz; 41.75.Ht

Coherent X-ray sources have important applications in biology, chemistry, condensed matter physics, and material science. In recent years, there is growing interest in generating single attosecond X-ray radiation pulse using Free Electron Lasers (FELs) [1–8]. In this paper we propose a scheme to generate density modulation at X-ray wavelength with application to producing single attosecond pulse coherent X-ray radiation. This scheme compresses the initial seeded energy modulation wavelength inside the electron beam by a factor of M, $M = 1+h_b R^a_{56}$. This compression factor can be made as large as a few hundreds by using a laser chirper and two bunch compressors to reach the final short-wavelength modulation. It differs from other FEL seeding schemes that make use of harmonics of the seeded modulation wavelength to reach short-wavelength radiation [9–11], even though the harmonics of the compressed modulation in the proposed scheme can still be used. This makes the final radiation wavelength and pulse length from the proposed scheme tunable by adjusting the compression factor and the laser parameters. The proposed scheme also has significant advantages over our previously proposed compression scheme [12] [1], where the final modulation compression factor is C instead of M. Here, C is the compression factor from the first bunch compressor. For a final compression factor of hundreds as proposed in this paper, a small jitter of the initial beam energy chirp will result in a large change of the compression factor. In contrast to those previous schemes, this new scheme does not suffer from jitter largely as will be explained later. The new scheme also simplifies the hardware layout by using one fewer laser modulator and makes the whole scheme more compact than the previous scheme.

FIG. 1: A schematic plot of the lattice layout of the modulation compression scheme.

A schematic plot of the modulation compression scheme is given in Fig. 1. It consists of an energy chirped electron beam, a seeding laser modulator, a bunch compressor A, a laser chirper, and another bunch compressor B. In this scheme, an energy chirped electron beam is sent into the seeding laser modulator to obtain initial energy modulation. By doing the energy chirping first instead of energy modulation first, it avoids the potential distortion of the modulation from collective effects during the process of chirping inside the linac. This also allows one to use the full linac to generate the initial energy-bunch length chirp. This is in contrast to most of the currently operating XFELs and those under design, where the residual energy chirp after the bunch compression has to be removed by running the electron bunch off crest after the bunch compressor. This makes the acceleration less effective. Inserting a chicane with a reasonable compression factor inside such a linac will produce the same amount of chirp required in this compression scheme and will reduce the total voltage needed from the linac by a factor of the compression factor. For an electron with initial longitudinal coordinates (z_0, δ_0) before chirping, where z is the relative longitudinal distance with respect to the reference particle, and $\delta = \Delta E/E$ is the relative energy deviation, the energy after the chirping and the first laser modulation will be:

$$\delta_2 = \delta_1 + A\frac{1}{1+\delta_1}\frac{\sin(4N_w\delta_1\pi)}{4N_w\delta_1\pi}\sin(kz) \qquad (1)$$

*Electronic address: jqiang@lbl.gov

[1] A similar scheme to Ref. [12] using accelerator chirpers was also independently proposed by Ratner et al. [13, 14].

where $\delta_1 = \delta_0 + h\ z$ represents the relative energy spread after chirping from the linac, where h is the energy chirp associated with the electron beam before the first bunch compressor, A is the modulation amplitude in the unit of the relative energy, N_w is the number of periods of the wiggler in the laser modulator, and k is the wave number of the seeding laser. Given the fact that the bunch length is normally below a millimeter, the required initial chirp for the first bunch compressor is on the order of tens m^{-1}, and the number of wiggler periods is small, then Eq. (1) can be approximated as:

$$\delta_2 \ = \ \delta_1 + A\sin(kz). \tag{2}$$

Assume the longitudinal phase space distribution after the laser energy modulation as $F(z, (\delta - hz - A\sin(kz))/\sigma)$, after the beam transports through the bunch compressor A, the laser chirper, and the bunch compressor B, the final longitudinal phase space distribution will be:

$$\begin{aligned} f(z,\delta) \ = \ & F\left(Mz - (R^b_{56}M + R^a_{56})\delta,\right. \\ & [\delta(1 + hR^a_{56} + (h_b + hM)R^b_{56}) - (h_b + hM)z - \\ & \left. A\sin(kMz - k(R^b_{56}M + R^a_{56})\delta)]/\sigma\right) \end{aligned} \tag{3}$$

where

$$M \ = \ 1 + h_b R^a_{56} \tag{4}$$

denotes the total final modulation compression factor, R^b_{56} is the momentum compaction factor of the second bunch compressor, and σ is the beam uncorrelated energy spread. If the chirp h_b introduced by the laser chirper is $-hC$, i.e. $h_b = -hC$, the total modulation compression factor M will be C, i.e. $M = C$. If the beam is over unchirped inside the laser chirper, i.e. $h_b = (-h + \tilde{h})C$, the total modulation compression factor will be $M = (1 + \tilde{h}R^a_{56})C$. Here, "over unchirp" means not only to remove the original energy chirp of the beam after the bunch compressor A but also to introduce another energy chirp to the beam in the opposite direction to the original chirp. This improves the final compression factor in the new scheme by a factor of $1 + \tilde{h}R^a_{56}$, where the $\tilde{h}$ stands for the extent of over unchirping of the initial chirp inside the laser chirper. It is also seen from Eq. 4 that the final modulation compression factor does not depend on the initial beam energy chirp jitter. Meanwhile, using a lower compression factor (~ 10) from the first bunch compressor while maintaining the same final compression factor (~ 100), the final beam current can also be made not sensitive to the beam energy chirp jitter. By properly choosing the momentum compaction factor of the second bunch compressor, i.e.

$$R^b_{56} = -R^a_{56}/M, \tag{5}$$

the final longitudinal phase space distribution is reduced into:

$$f(z,\delta) \ = \ F(Mz, [\delta - M\tilde{h}z - MA\sin(kMz)]/M\sigma) \tag{6}$$

The above distribution function represents a compressed modulation in a chirped beam. It should be noted that the momentum compaction factor of the second bunch compressor does not have to be opposite sign with respect to the first bunch compressor if the total compression factor M, i.e. C or $1 + \tilde{h}R^a_{56}$, is made negative. In the above equations, we have also assumed a longitudinally frozen electron beam and a linear laser chirper instead of the actual sinusoidal function from the laser modulator. The effects of sinusoidal energy modulation from the laser chirper will be discussed below.

To generate a large energy chirping amplitude in the chirper after the first bunch compressor is not easily accessible using a conventional RF linac structure. Using a laser modulator, this chirp can be easily achieved by taking advantage of the short wavelength and the high power of the laser. The disadvantage of using such a laser chirper is that not the whole electron beam will be uniformly unchirped due to the sinusoidal form of the energy modulation. Only periodically separated local segments of the beam will be correctly unchirped. However, such a property can be used to generate ultra-short coherent X-ray radiation by controlling the fraction of the beam that can be properly unchirped using a few-cycle laser pulse with carrier envelope phase stabilization. In the following simulation, we will produce such an attosecond short-wavelength modulated beam as an illustration.

The parameters of the electron beam and the lattice are summarized in Table I. Here, a short uniform electron bunch (100 μm) with 20 pC charge, 2 GeV energy, -23.95 m^{-1} energy-bunch length chirp, and an uncorrelated energy spread of 1×10^{-6} is assumed at the beginning of the laser modulator. The initial normalized modulation amplitude A is 1.2×10^{-6}. Assuming 1 Tesla magnetic field in the wiggler with a total length of 33 cm and a period of 11 cm, this corresponds to about 130 kW 200 nm wavelength laser power. After the modulator, we add an uncorrelated energy spread of 0.56 keV to account for the synchrotron radiation effects inside the wiggler magnet using an estimate from Refs. [8, 15]. Af-

TABLE I: Electron beam and lattice parameters in the illustration example

beam energy (GeV)	2
beam current (A)	60
initial enegy chirp (/m)	-23.95
initial relative energy spread	10^{-6}
laser modulation amplitude (10^{-6})	1.2
laser modulator wavelength (nm)	200
laser modulator power (kW)	130
R_{56} of bunch compressor A (cm)	4
laser chirp amplitude (10^{-4})	1.58
laser chirp wavelength (nm)	200
laser chirp power (GW)	2
R_{56} of bunch compressor B (mm)	-0.2

ter the initial seeding laser modulator, the beam passes through a chicane bunch compressor. Here, we have assumed that the R_{56} of the chicane is about 4 cm. As the electron beam passes through a bending magnet, the quantum fluctuation of the incoherent synchrotron radiation (ISR) could cause the growth of the uncorrelated energy spread. Such a growth of the uncorrelated energy spread might smear out the modulation signal after the compression. Here, we assume four 4 meter long bending magnets inside the chicane each with 0.0655 radian bending angle in order to reduce the growth of the uncorrelated energy spread. The rms energy spread induced by the ISR through such a chicane is about 0.44 keV using an estimate from Refs. [8, 16]. After the beam passes through this bunch compressor, the total bunch length of the beam is compressed down to about 4 μm due to a factor of 25 compression from the first bunch compressor. This beam is transported through another few-cycle laser modulator with 200 nm resonance wavelength. This modulator works as an unchirper to remove the correlated energy chirp along the beam. Here, the normalized amplitude of the laser is chosen as 1.58×10^{-4} so that the total modulation compression factor at the end of the second bunch compressor is about 200. This modulation amplitude corresponds to about 2 GW laser power using the same wiggler as the first laser modulator. After the beam transports through the laser modulator chirper, it passes through a dog-leg type bunch compressor that can provide opposite sign R^b_{56} compared to the chicane. For a total compression factor of 200 in this example, the R^b_{56} for the second bunch compressor is about -0.2 mm. Figure 2 shows the longitudinal phase space of the beam at the end of the second bunch compressor. It is seen that after the second bunch compressor, only a small fraction of beam is locally unchirped and further compressed. This also makes the above scheme less sensitive to the time jitter between the laser and the electron beam. The final energy spread in that zoom-in small section of the beam is also small and good for generating coherent X-ray radiation in an undulator radiator downstream. Figure 3 shows the projected current profile for this prebunched beam. Given the initial 60 A current, the central prebunched current peak with 1 nm wavelength modulation reaches 5.5 kA after the above compression scheme. There are other lower current spikes besides the central peak inside the beam. Those spikes will not contribute significantly to the final 1 nm attosecond radiation since density microbunching in those spikes is very small due to fact that the energy chirp at those locations does not produce correct compression factor to satisty the Eq. 5 of the two bunch compressors. The length of the central prebunched beam is about a hundred attoseconds. It is set by the half wavelength of the laser chirper. Such a highly prebunched beam can be used to generate coherent attosecond X-ray radiation in a short undulator.

To study the detailed radiation process and the radiation properties, we use the GENESIS simulation code [17] to calculate the coherent X-ray radiation through a short

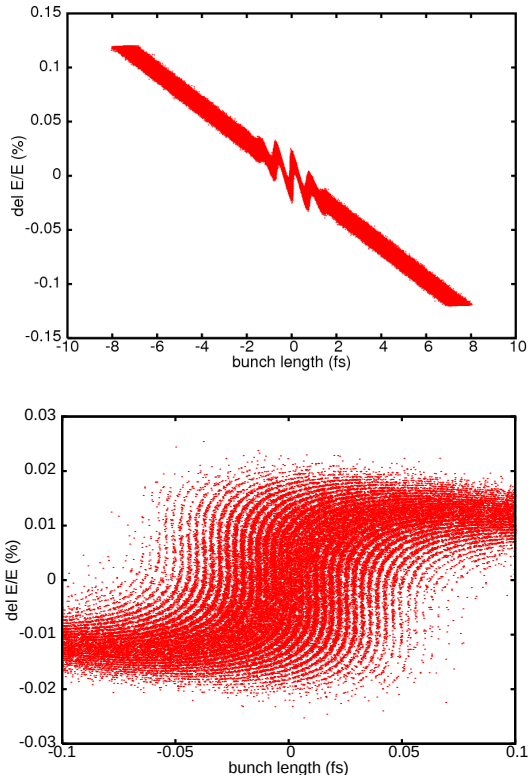

FIG. 2: Longitudinal phase space after the compression scheme (top) and the zoom-in phase space around the center of the beam (bottom).

undulator radiator. The normalized emittance of the electron beam is chosen to be 0.2 μm. The length of the radiator is 1.5 m with an undulator period of 1.5 cm. The details of the radiation properties at the end of the undulator are shown in Fig. 4, where the radiation pulse power temporal profile is shown as the top subplot and the radiation pulse spectral profile is shown as the bottom subplot. The profiles are fit to Gaussian curves which give a temporal rms size of 71.3 as and a spectral rms width of 4.2 pm. This results in a phase space area of about 0.56, which is close to the transform limit of the X-ray pulse. The full width at half maximum of the radiation pulse is about 170 as, which is larger than the width of the central modulated current density distribution. This is due to the slippage of the photon pulse with respect to the electron bunch inside the radiator.

In this paper, we proposed a scheme to generate attosecond coherent X-ray radiation through modulation compression. This scheme allows one to tune the final X-ray radiation wavelength by adjusting the compression factor. It also allows one to control the final radiation pulse length by controlling the laser chirper parameters and the initial compression parameters. The proposed scheme requires a small initial seeding laser power due to compression amplification. This makes it possible to use the relatively low power ($\sim$ 100 kW) and shorter wavelength laser ($\sim$ 10 nm) from the higher-order harmonic

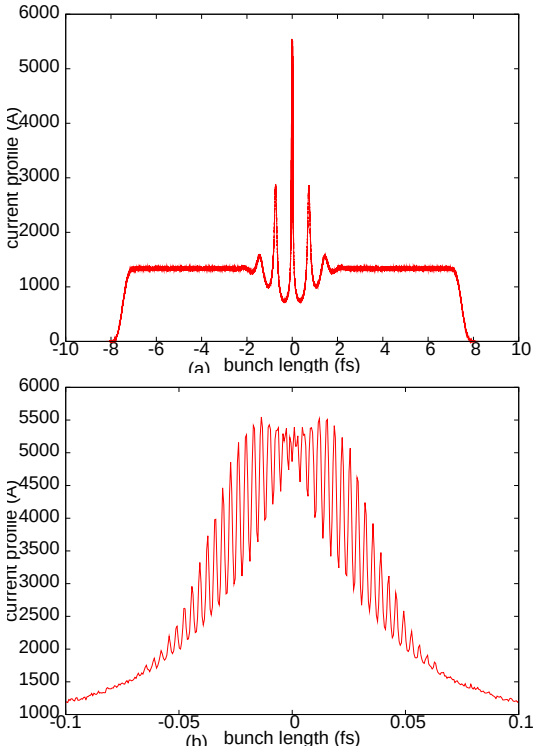

FIG. 3: Beam current distribution after the compression scheme (a) and the zoom-in current distribution around the center of the beam (b).

generation (HHG) scheme to seed the electron beam before the first bunch compressor [18]. This could result in a prebunched beam with a modulation wavelength down to the hard X-ray regime using the above single stage compression scheme. The high compression factor in the proposed scheme also lowers the required initial current in order to achieve final kilo-Ampere electron beam current. This helps maintain good beam quality transporting through the linear accelerator. In the above illustration example, a single 1 nm attosecond pulse is generated with a 200 nm laser seeded 60 Ampere current beam. Another laser chirper, bunch compressor and radiator can be added after the first X-ray radiator to generate a second attosecond pulse with different radiation wavelength using another part of the beam to achieve two-color option [8]. Also, in this example, we assumed an opposite-sign second bunch compressor. By tuning the laser chirper parameters, the momentum compaction factor of the second bunch compressor can have the same sign as the first bunch compressor. In this case, another chicane can be used in the above scheme to generate the attosecond coherent X-ray radiation as suggested in Reference [13] by using an over compressed beam in the first bunch compressor.

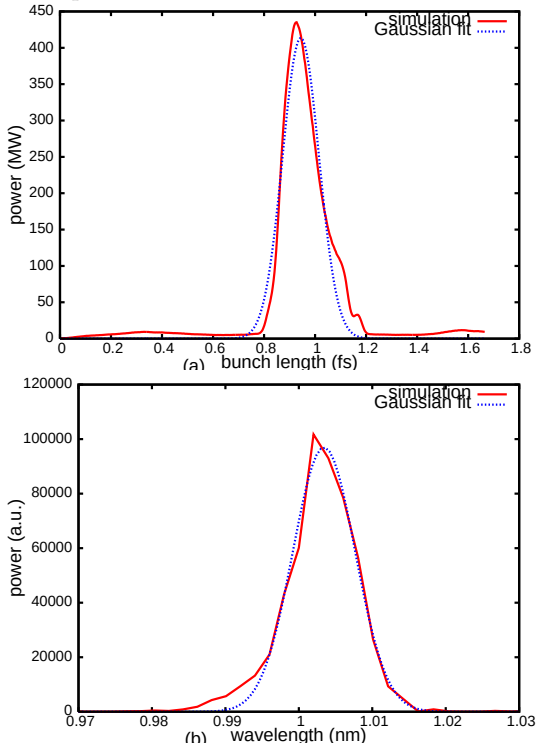

FIG. 4: The radiation pulse temporal profile (a) at the end of the 1.5 m long undulator and the radiation pulse spectral profile (b) at the end of the 1.5 m long undulator.

Acknowledgments

We would like to thank Drs. J. Corlett, Y. Ding, B. Fawley, Z. Huang, R. Ryne, R. Wilcox, D. Xiang, S. Zhang, and A. Zholents for useful discussions. We would also like to thank Mr. W. Tabler for helping improve the readability of the paper. This research used computer resources at the National Energy Research Scientific Computing Center and at the National Center for Computational Sciences. The work of JQ was supported by the U.S. Department of Energy under Contract No. DE-AC02-05CH11231 and the work of JW was supported by the U.S. Department of Energy under contract DE-AC02-76SF00515.

[1] A.A. Zholents and W.M. Fawley, Phys. Rev. Lett. **92**, 224801 (2004).
[2] A.A. Zholents and G. Penn, Phys. Rev. ST Accel. Beams **8**, 050704 (2005)
[3] E.L. Saldin, E.A. Schneidmiller, and M.V. Yurkov, Phys. Rev. ST Accel. Beams **9**, 050702 (2006)
[4] J. Wu, P.R. Bolton, J.B. Murphy, K. Wang, Optics Express **15**, 12749, (2007).
[5] A.A. Zholents and M.S. Zolotorev, New Journal of Physcis **10**, 025005 (2008).

[6] Y. Ding, et al., Phys. Rev. ST Accel. Beams **12**, 060703 (2009).
[7] D. Xiang, Z. Huang, and G. Stupakov, Phys. Rev. ST Accel. Beams **12**, 060701 (2009).
[8] A.A. Zholents and G. Penn, Nucl. Instr. Meth. A **612**, 254 (2010).
[9] L. Yu, Phys. Rev. A **44**, 5178 (1991).
[10] T. Shaftan and L. Yu, Phys. Rev. E **71**, 046501 (2005).
[11] G. Stupakov, Phys. Rev. Lett **102**, 074801 (2009).
[12] J. Qiang, Nucl. Instr. and Meth. A **621**, 39 (2010).
[13] D. Ratner, Z. Huang, A. Chao, in proceedings of 31^{st} International Free Electron Laser Conference, Liverpool, UK, August 23-28, 2009, p. 200.
[14] D. Ratner, Z. Huang, A. Chao, Phys. Rev. ST Accel. Beams **14**, 020701 (2011).
[15] E. Saldin, E. Schneidmiller, M. Yurkov, Nucl. Instr. and Meth. A **381**, 545 (1996).
[16] A.W. Chao, M. Tigner, *Handbook of Accelerator Physics and Engineering*, World Scientific, Singapore, 2006.
[17] S. Reiche, Nucl. Instr. and Meth. A **429**, 243 (1999).
[18] E. J. Takahashi, et al., Appl Phys. Letts. **84**, p. 4 (2004).